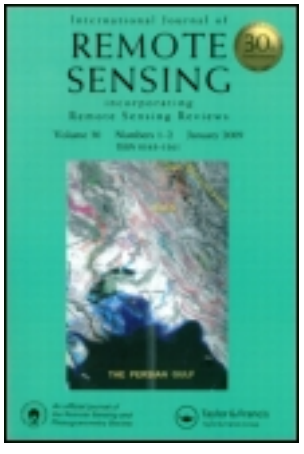

International Journal of Remote Sensing
Publication details, including instructions for authors and subscription information:
http://www.tandfonline.com/loi/tres20

A comparison of three methods for estimating the LAI of black locust (Robinia pseudoacacia L.) plantations on the Loess Plateau, China

Jing-Jing Zhou[a], Zhong Zhao[a], Jun Zhao[a], Qingxia Zhao[a], Fei Wang[a] & Haize Wang[a]
[a] Key Laboratory of Environment and Ecology in Western China of Ministry of Education, College of Forestry, Northwest A & F University, Yangling, Shaanxi 712100, PR China
Published online: 24 Dec 2013.

To cite this article: Jing-Jing Zhou, Zhong Zhao, Jun Zhao, Qingxia Zhao, Fei Wang & Haize Wang (2014) A comparison of three methods for estimating the LAI of black locust (Robinia pseudoacacia L.) plantations on the Loess Plateau, China, International Journal of Remote Sensing, 35:1, 171-188, DOI: 10.1080/01431161.2013.866289

To link to this article: http://dx.doi.org/10.1080/01431161.2013.866289

International Journal of Remote Sensing, 2014
Vol. 35, No. 1, 171–188, http://dx.doi.org/10.1080/01431161.2013.866289

Taylor & Francis
Taylor & Francis Group

A comparison of three methods for estimating the LAI of black locust (*Robinia pseudoacacia* L.) plantations on the Loess Plateau, China

Jing-Jing Zhou, Zhong Zhao*, Jun Zhao, Qingxia Zhao, Fei Wang, and Haize Wang

Key Laboratory of Environment and Ecology in Western China of Ministry of Education, College of Forestry, Northwest A & F University, Yangling, Shaanxi 712100, PR China

(*Received 21 November 2012; accepted 22 October 2013*)

Optical remote sensing is the most widely used method for obtaining leaf area index (LAI) information. However, there is a need for improved processing techniques to increase the accuracy of LAI estimates obtained in this way. This article describes the use of high-resolution optical data from the Quickbird satellite for LAI estimation in the semi-arid region of the Loess Plateau, China. Three different image processing techniques were evaluated: processing based on spectral vegetation indices (SVIs), texture parameters, and combinations of SVIs with textural analyses. Simple linear and nonlinear regression models were developed to describe the relationship between image parameters obtained using these approaches and 52 field measurements of LAI. SVI-based approaches did not yield reliable LAI estimates, accounting for at best 68% of the observed variation in LAI. Texture-based methods were somewhat better, explaining up to 72% of the observed variation. A combination of the two approaches yielded an even better adjusted r^2 value of 0.84. This demonstrates that the accuracy of estimated LAI values based on remote-sensing data can be significantly increased by considering a combination of SVIs and texture parameters.

Keywords: LAI; texture parameters; vegetation index; black locust (*Robinia pseudoacacia* L.); Quickbird image

1. Introduction

Leaf area index (LAI) is an important descriptor of vegetation conditions that is widely used in physiological and biogeochemical studies (Asner et al. 1998). It is not only the most important biophysical variable characterizing vegetation abundance and distribution across the landscape (Gray and Song 2012), but is also a part of the essential climate variable identified by the Global Climate Observing System (GCOS 2006). The establishment of an exact estimation method of LAI is to evaluate the forest biomass (Solana-Arellano, Echavarria-Heras, and Martinez 2003; Tobin et al. 2006) and the impacts of environment deterioration (Shin et al. 2010). Remote-sensing technologies have become increasingly important in large-scale ecological studies due to their low cost and ability to rapidly provide large amounts of relevant information. A number of publications have described the use of remote-sensing techniques for mapping forest parameters such as age, height, LAI, and biomass using optical methods (Boyd 1999; Fassnacht et al. 1997; Muukkonen and Heiskanen 2005; Wolter, Townsend, and Sturtevant 2009), synthetic aperture radar (SAR) (Canisius and Fernandes 2012), and lidar (Fu et al. 2011; Korhonen et al. 2011; Thomas et al. 2011; Zhao et al. 2011). Although various remote-

*Corresponding author. Email: zhaozhlunwen2010@126.com

sensing techniques for quantifying LAI have been evaluated, a broadly applicable method that is suitable for use on regional scales has not yet been identified, largely due to the broad diversity of forest ecosystems in terms of their environmental, topographic, and biophysical properties (Sarker and Nichol 2011).

The Loess Plateau of China is located in the middle of the Yellow River basin and has suffered serious environmental problems relating to soil erosion and ecosystem degradation. To address these issues, the Chinese government has launched a number of large-scale vegetation restoration programmes (Cao, Chen, and Yu 2009). The black locust (*Robinia pseudoacacia* L.) is the most abundant tree species on the Loess Plateau and has been widely planted. This is due to its advantageous characteristics, which include rapid growth, drought tolerance, shade intolerance, nitrogen fixation, and utility as a source of timber and fuel (Burner, Pote, and Ares 2005; Wang et al. 2009; Wei et al. 2009). Until now, however, little work has been done on estimating the LAI of black locust trees growing in the Loess Plateau region.

The vegetation index is a measure that is widely used in conjunction with optical remote-sensing methods for measuring LAI. It is usually calculated based on an analysis of the ratio of red and near-infrared light reflected from the area of land under study to determine the spectral contribution from green vegetation. LAI data can be obtained by analysing optical data using regression models based on spectral vegetation indices (SVIs). Such analyses do not require additional geometric information on the area of land being analysed and minimize contributions from the soil background, angle of the sun, sensor view angle, senesced vegetation, and the atmosphere (Huete, Jackson, and Post 1985). However, the dynamic nature of forests limits the accuracy of LAI estimates based on observations of a single variable. Factors such as differences in crown closure, shadows, and stand density can produce markedly different stand structures that nevertheless yield identical vegetation index values (Wulder et al. 1998). Moreover, the relationships between LAI and SVIs show saturation when LAI values are greater than 3–5, which is one of the principal limitations of remote sensing of LAI in forest canopies (Davi et al. 2006).

Image texture analysis involves measuring heterogeneity in the tonal values of pixels within a defined area of an image (Wood et al. 2012) and can be used to identify objects or regions of interest (Haralick, Shanmugam, and Dinstein 1973). Images with high spatial resolution can potentially provide more textural information than low-resolution data because they make it possible to distinguish the finer structure of the studied forests (Wulder et al. 1998; Tuominen and Pekkarinen 2005). However, texture is a very complex parameter and is highly sensitive to the object under study, the physiographic conditions, and the window size employed (Marceau et al. 1990; Chen and Cihlar 1996; Franklin, Wulder, and Lavigne 1996). Texture has been used to estimate forest structure parameters (Kayitakire, Hamel, and Defourny 2006; Ozdemir and Karnieli 2011) and as an input for vegetation classification (Aguera, Aguilar, and Aguilar 2008; Kabir et al. 2010; Ota, Mizoue, and Yoshida 2011).

The accuracy of LAI estimates based on remote-sensing data could potentially be improved by incorporating textural information into SVIs, especially for LAI values greater than 3 (Wulder 1998; Wulder et al. 1998). Colombo et al. (2003) reported that incorporating dissimilarity information into the NDVI improved the fit of the regression equation for most vegetation types relative to that achieved using SVIs alone. Gu et al. (2012) used spectral and spatial information from IKONOS-2 images to retrieve LAI values for urban forests. They found that for natural broadleaved forests (which are both dense and spatially complex), combining VI with texture improved the accuracy of the retrieved LAI values by between 8.9% and 27.0% relative to that achieved using the vegetation index alone. However, to our knowledge, few studies have directly evaluated

the combined use of SVIs and textural information for estimating LAI values in mountain areas.

Therefore, the objectives of this study were (i) to assess the potential of Quickbird data used for estimating LAI values of black locust plantations in mountain areas of the Loess Plateau in China and (ii) to compare the performance of three methods for retrieving LAI data and their sensitivity: SVI-based image processing, texture-based processing, and a combination of SVI- and texture-based processing. The results obtained provide important information on the performance of different methods for estimating LAI values for black locust trees in the Loess Plateau and on the use of textural information derived from remote-sensing data in LAI modelling.

2. Study area and data

2.1. Study area

All LAI measurements were taken within the experimental area known as Huaiping forest farm (34° 47′–34° 51′ N and 108° 05′–108° 10′E), whose elevation ranges from 1123 to 1417 m above sea level. It is located in Yongshou County of Shaanxi Province on the Loess Plateau of China. The region has an annual mean temperature ranging from 7.0°C to 13.3°C (Luo 1995) and an annual mean precipitation of 600.6 mm, of which 53% falls between July and September (Peng, Zhong, and Zhan-bin 2004; Zhong et al. 2006). The local growing season usually starts in early April and lasts until late October. Seventy-six sample plots were selected; their locations are shown on the Quickbird panchromatic image in Figure 1. Fifty-two samples were then selected at random and used to develop linear and nonlinear regression models. The remaining 24 samples were used to test the robustness of the developed models.

2.2. Data

This study was based on a single Quickbird panchromatic-multispectral image that was acquired on 22 June 2012 under clear sky conditions. The panchromatic image has a spatial resolution of 0.6 m while the resolution of the multispectral image is 2.4 m. The solar azimuth angle was 108.3° and the solar elevation angle was 66.1°. The multispectral image covers four wavebands corresponding to blue (450–520 mm), green (520–600 nm), red (630–690 mm), and near-infrared (760–890 mm).

3. Methods

The LAI estimates obtained by analysis of remote-sensing data were compared to field LAI measurements. Plot LAI data were obtained from field measurements of 76 sample plots. Image parameters based on SVIs, texture parameters, and a combination of the two were extracted for all field plots using an area of interest mask (AOI) of 20 m × 20 m. LAI data for each field plot were then used as independent variables with the image parameters as dependent variables in simple linear and nonlinear models.

3.1. Ground-based LAI measurements

The LAI-2200 instrument (LI-COR Inc., Lincoln, NE, USA; Li-Cor, 2010) was used to indirectly measure LAI in 76 black locust plantation plots. LAI measurements were performed on 16 June and 15 July 2012, under diffuse radiation conditions at sunrise and sunset using a single sensor. At each site, two above-canopy and nine low-canopy readings (see Figure 2)

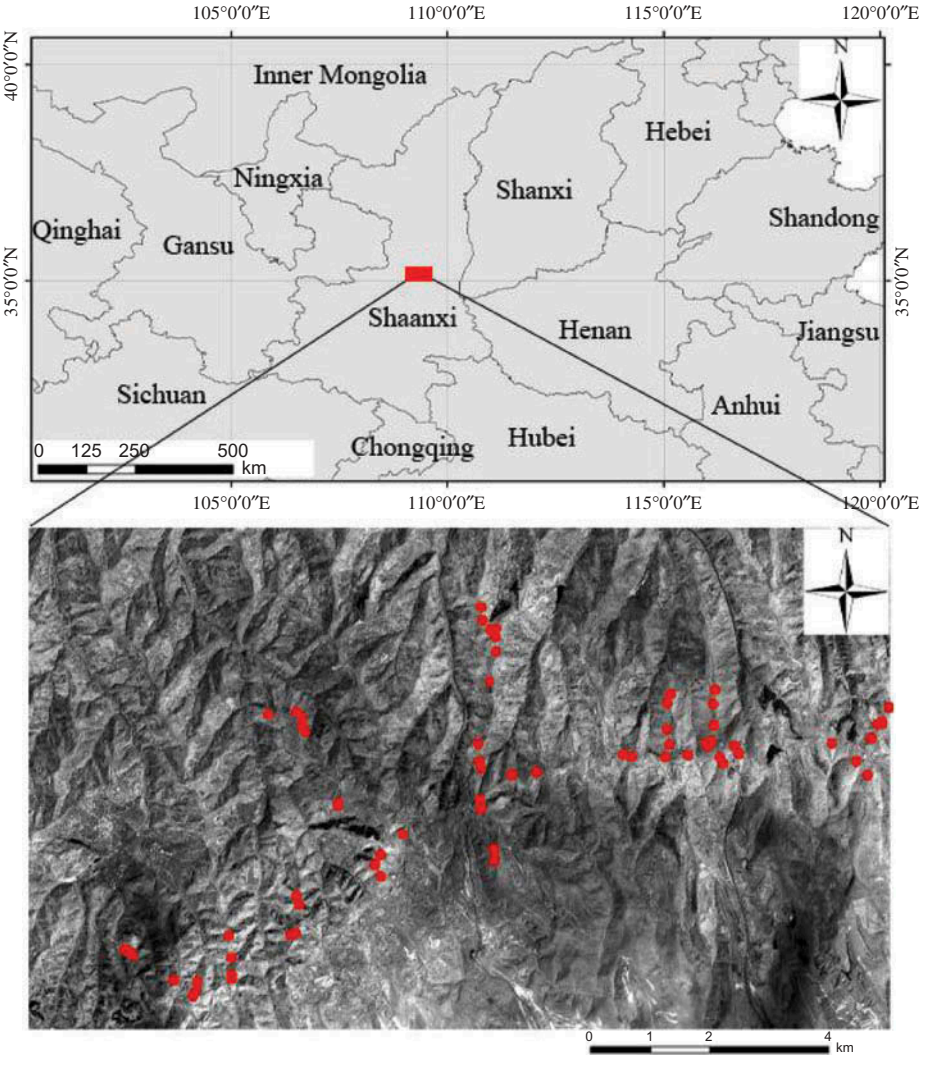

Figure 1. A portion of the study area and the location of the sample plots in the Loess Plateau region of Yongshou County, Shaanxi Province, China.

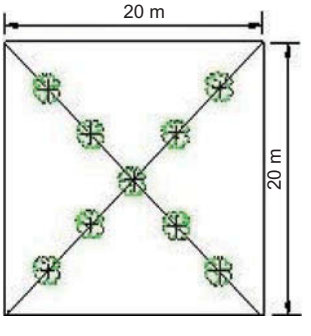

Figure 2. Distribution of sampling points within each plot.

were taken with an opaque, 180° view-restricting cap (Jonckheere et al. 2004; Soudani et al. 2006) placed over the sensor in order to mask out the operator. In keeping with the recommendation of Chason, Baldocchi, and Huston (1991), ring 5 was excluded in these analyses in order to obtain the most accurate LAI estimates possible. This was found to improve the agreement between the estimates and direct measurements based on litter trap results.

3.2. *Remote-sensing data – pre-processing and estimating reflectance*

Orthorectification of the panchromatic data was performed using the ENVI 4.7 software package (Exelis Visual Information Solutions, Boulder, CO, USA). Fifty well-distributed ground control points (GCPs) and a high-resolution (1:10000) digital elevation model were used, and the overall error was 0.68 pixels. We then used the corrected panchromatic data to rectify the multispectral data, giving an overall error of 0.34 pixels. The raw digital number value for the multispectral data was converted to spectral radiance and subsequently to top of atmosphere (TOA) reflectance. Atmospheric correction was performed using the Fast Line-of-sight Atmospheric Analysis of Spectral Hypercubes (FLAASH) approach (Yuan, Niu, and Wang 2009).

3.3. *Vegetation indices*

A vegetation index simply expresses the image values observed in two or more wavebands as a single value that is related to a biophysical variable of interest (Mather 1999). The average reflectance data for each plot were used to compute a range of vegetation indices, as shown in Table 1. NDVI is the most widely used vegetation index in remote-

Table 1. Selected SVIs used for LAI estimation.

Index	References
Simple ratio (SR)$=\frac{\mathrm{NIR}}{\mathrm{R}}$	Jordan (1969)
Soil-adjusted vegetation index (SAVI) $= (1+\mathrm{L})\frac{(\mathrm{NIR}-\mathrm{R})}{(\mathrm{NIR}+\mathrm{R}+\mathrm{L})}$	Huete (1988)
Enhanced vegetation index (EVI) $= \mathrm{G}\frac{(\mathrm{NIR}-\mathrm{R})}{(\mathrm{NIR}+\mathrm{C1NIR}-\mathrm{C2B}+\mathrm{C3})}$	Huete, Justice, and Liu (1994)
Atmospherically resistant vegetation index (ARVI) $=\frac{\mathrm{NIR}-\mathrm{R}}{\mathrm{NIR}+\mathrm{RB}}$	Kaufman and Tanre (1992)
Vegetation index (RB) = NIR – γ(B – R)	
Modified soil-adjusted vegetation index (MSAVI) $= \left[(2\mathrm{NIR}+1)-\sqrt{(2\mathrm{NIR}+1)^2-8(\mathrm{NIR}-\mathrm{R})}\right]/2$	Qi et al. (1994)
Non-linear vegetation index (NLI) $=\frac{\mathrm{NIR}^2-\mathrm{R}}{\mathrm{NIR}^2+\mathrm{R}}$	Gong et al. (2003); Goel and Qin (1994)
Difference vegetation index (DVI) = NIR – R	Richardson and Wiegand (1977)
Normalized difference vegetation index (NDVI) $=\frac{\mathrm{NIR}-\mathrm{R}}{\mathrm{NIR}+\mathrm{R}}$	Rouse et al. (1974)

Notes: B, R, and NIR represent Quickbird reflectance in the blue, red, and near-infrared wavelengths, respectively. Parameters L and γ represent the SAVI term (set to 0.5) and the ARVI term (set to 1), respectively. The coefficients used in the EVI algorithm are C1 = 6.0, C2 = 7.5, C3 = 1, and G = 2.5 (Comombo et al. 2003).

sensing applications and was therefore used as a reference when evaluating the performance of the texture-based method (Rouse et al. 1974). The correlation between the LAI estimates obtained with different SVIs and those obtained from the ground measurements was analysed. Only SVIs with an adjusted r^2 value of >0.55 for this relationship (Table 3) were tested in conjunction with textural data; the SVIs that satisfied this criterion were difference vegetation index (DVI), enhanced vegetation index (EVI), normalized difference vegetation index (NDVI), soil-adjusted vegetation index (SAVI), and modified soil-adjusted vegetation index (MSAVI) (see Section 3.5).

3.4. *Texture analysis*

Texture indices (Table 2) were calculated based on the Quickbird panchromatic band at the maximum spatial resolution of 0.60 m using the grey-level co-occurrence matrix (GLCM) method together with grey-level difference vector (GLDV)-based texture measurements. The use of a small window size is known to exaggerate differences within the window but retains high spatial resolution, whereas larger windows may cause inefficient extraction of texture information due to over-smoothing of textural variations (Nichol and Sarker 2011; Sarker and Nichol 2011). Therefore, to obtain accurate information on the texture of the vegetation, four different window sizes were tested (3 × 3, 5 × 5, 7 × 7, and 9 × 9 pixels) for each texture parameter considered. In each case, the window size that yielded the highest adjusted r^2 value for the specific parameter in question was used when computing LAI estimates based on both an SVI and a texture parameter.

Table 2. Textural parameters considered in this work (Haralick, Shanmugam, and Dinstein 1973).

Grey-level co-occurrence matrix (GLCM)-based texture parameter estimation
Mean (ME) $= \sum_{i,j=0}^{N-1} iPi,j$
Homogeneity (HOM) $= \sum_{i,j=0}^{N-1} i\frac{P_{ij}}{1+(i-j)^2}$
Contrast (CON) $= \sum_{i,j=0}^{N-1} iP_{i,j}(i-j)^2$
Dissimilarity (DIS) $= \sum_{i,j=0}^{N-1} iPi,j\lvert i-j\rvert$
Entropy (ENT) $= \sum_{i,j=0}^{N-1} iPi,j(-\mathrm{In}Pi,j)$
Variance (VAR) $= \frac{\sum_{i,j}\left(x_{ij}-\mu\right)^2}{n-1}$
Angular second moment (ASM) $= \sum_{i,j=0}^{N-1} iPi,j^2$
Correlation (COR) $= \frac{\sum_{i,j=0}^{N-1} iP_{i,j}-\mu 1\mu 2}{\sigma 1^2\sigma 2^2}$
$\mu_1 = \sum_{i=0}^{N-1} i\sum_{j=0}^{N-1} Pi,j$
$\mu_2 = \sum_{j=0}^{N-1} j\sum_{j=0}^{N-1} Pi,j$
$\sigma_1^2 = \sum_{i=0}^{N-1} (i-\mu 1)^2\sum_{j=0}^{N-1} Pi,j$
$\sigma_2^2 = \sum_{j=0}^{N-1} (j-\mu 1)^2\sum_{i=0}^{N-1} Pi,j$
Here, $P(i, j)$ is the normalized co-occurrence matrix.

3.5. Combined SVIs and texture parameters

All textural images were resampled to give a pixel size of 2.4m using nearest-neighbour resampling in order to integrate the texture information with the SVI results obtained from the multispectral image. Based on the results presented in Section 4.2, the window sizes used for the different textural parameters were 9 × 9 for DIS, 5 × 5 for CON and COR, and 3 × 3 for VAR, HOM, SEC, ASM, and ENT (see Table 2 for expansion of these abbreviations).

3.6. Statistical analysis

Empirical relationships between the image indices and LAI were investigated by performing linear and non-linear regression analyses using LAI as the independent variable and the image index as the dependent variable. Three common statistical parameters were considered to identify the most robust model with the best fit: the adjusted coefficient of determination (r^2), root mean square error (RMSE), and the p-level. Adjusted r^2 was computed based on either linear or nonlinear relationships between the two variables, as appropriate (Pu 2012). All statistical analyses were conducted using the SAS software package (version 8.0) for Windows (SAS Institute Inc., Cary, NC, USA).

4. Results and analysis

4.1. Performance of raw data processing and SVIs

The coefficients of determination for the relationships between field LAI values and spectral data for bands b1 (blue), b2 (green), and b3 (red) from the Quickbird data were found to be poor individually (Table 3). However, stronger correlations were observed for band 4 (near-infrared), for which the adjusted r^2 value was 0.66. Overall, the SVIs offered better performance than that achieved by simply looking at the reflectance from a single spectral band; the highest adjusted r^2 values were achieved using SAVI and MSAVI (0.68 in both cases). As mentioned in the Introduction, this improvement over analysis based on single bands is attributed to the ability of SVI-based analyses to enhance spectral

Table 3. The best results obtained from raw data processing and SVIs.

Variance	Model	r^2_{adj}	RMSE
b1	$y = 0.24 - 0.015x$	0.22	1.26
b2	$y = 0.41 - 0.025x$	0.34	1.20
b3	$y = 0.39 - 0.023bx$	0.19	1.10
b4	$y = 1.42 + 0.46x$	0.66	0.79
EVI	$y = 1.08 + 0.12x$	0.61	0.85
NLI	$y = 0.80 + 0.05x - 0.004x^2$	0.58	0.97
SR	$y = 9.42 + 0.86x$	0.34	1.06
DVI	$y = 1.69x^{0.49}$	0.56	0.90
SAVI	$y = 0.35x^{0.23}$	0.68	1.02
NDVI	$y = 0.68x^{0.14}$	0.67	1.02
ARVI	$y = 0.71 + 0.025x$	0.32	0.96
MSAVI	$y = 0.63 + 0.095x - 0.0084x^2$	0.68	0.91

Notes: The variables x and y in the above expressions represent the LAI values measured in the field and the spectral variables, respectively. All adjusted r^2 values are statistically significantly at the 0.99 confidence level. RMSE values were calculated based on the difference between measured and predicted LAI values.

contributions from green vegetation while minimizing those from soil background, sun angle, sensor view angle, senesced vegetation, and the atmosphere (Huete, Justice, and Liu 1994; Lu 2006).

4.2. *Performance of texture-processing methods*

The accuracy of the LAI estimates obtained by considering textural information within the Quickbird data was generally greater than that achieved using SVIs alone. The textural parameters that yielded the most accurate LAI estimates were entropy and the angular second moment, using 3 × 3 windows in both cases (Figure 3). Angular second moment, entropy, and homogeneity performed better than any other texture parameters whenever window size changed (Figure 3). It is important to note that the coefficient of determination between field data and predicted LAI values was significant for all models and variables ($p < 0.001$) with the exception of mean texture parameter (Figure 3).

The application of different window sizes did not influence the coefficient of determination for the relationships between textural parameters, and field LAI values for any parameter save the correlation index (Figure 4). However, in almost all cases, the r^2 values for window sizes of 3 × 3 and 5 × 5 were somewhat higher than those achieved with 7 × 7 or 9 × 9 windows (Figure 4). While the models based on the entropy and angular second

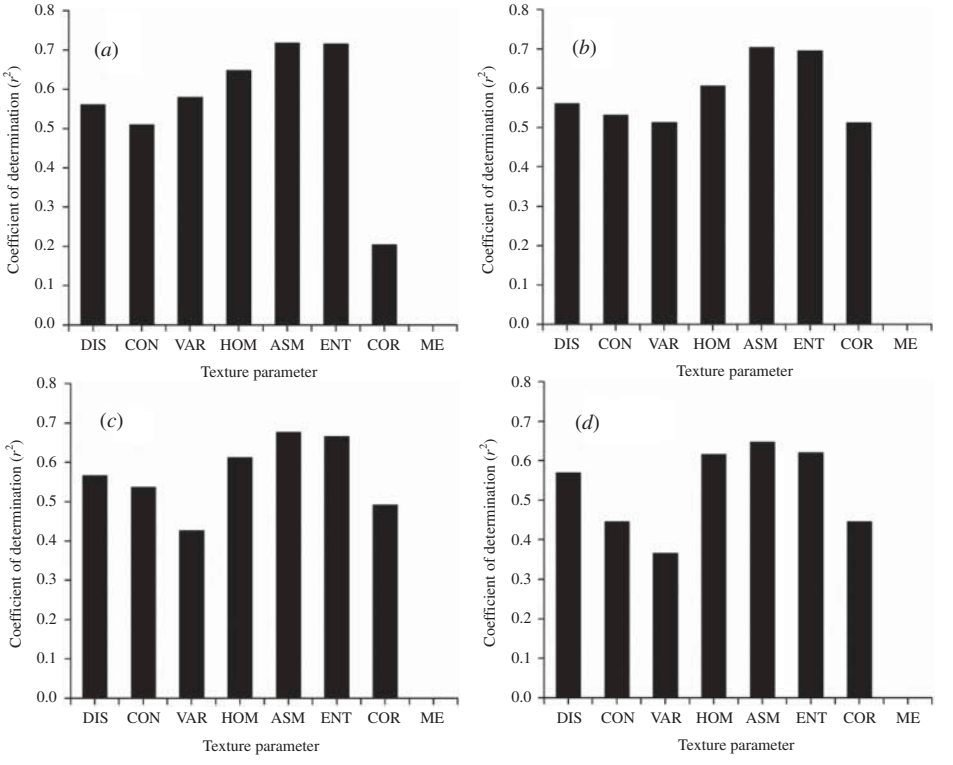

Figure 3. Accuracy of LAI estimates based on different texture parameters at various window sizes (subfigures (*a*), (*b*), (*c*), and (*d*) show the results obtained using window sizes of 3 × 3, 5 × 5, 7 × 7, and 9 × 9, respectively).

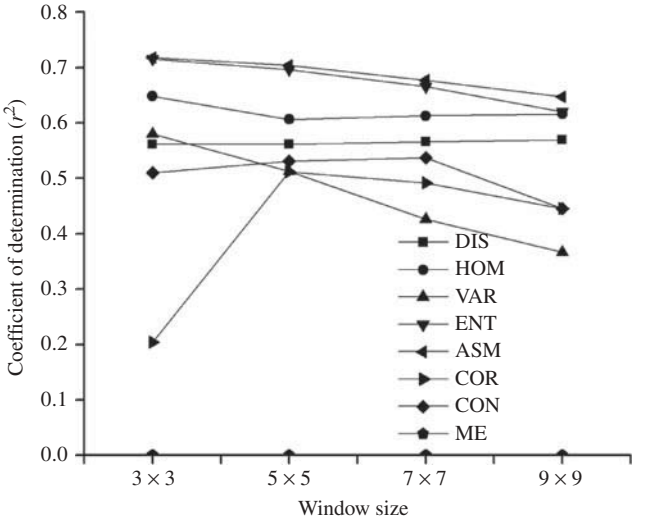

Figure 4. Coefficients of determination for relationships between LAI and texture parameters obtained using different window sizes.

moment texture parameters yielded better results than those achieved with the SVIs tested, even these models could only explain 72% of the observed variation in the field LAI data. Therefore, to obtain a more robust model for LAI estimation, we decided to explore the potential for using SVIs in conjunction with texture information to take full advantage of the richness of Quickbird data.

4.3. *Performance of SVIs in conjunction with texture parameters*

In most cases, the combination of an SVI with a texture parameter significantly improved the accuracy of the estimated LAI values (Table 4). The model based on a combination of angular second moment and MSAVI yielded the highest adjusted r^2 value observed in this work (Figures 5 and 6). This was a significant improvement in LAI estimation compared with the best result obtained using raw spectral band data, SVIs, and texture parameter models (Figure 7). Interestingly, the combination of entropy data with SVIs invariably yielded adjusted r^2 values that were lower than those achieved using entropy alone (Figure 7). In all cases, the results achieved using the models listed in Table 4 were statistically significant. Overall, these findings clearly demonstrate that the accuracy of LAI estimates can be improved by combining textural information with SVI-based analyses.

5. Discussion

Field measurements of LAI for black locust plantations in the Loess Plateau region were compared to spectral and textural indices calculated from high spatial resolution Quickbird images of the study area to identify effective methods for mapping LAI in this region by remote sensing. The relationships between measured LAI values and various spectral/textural indices were investigated using regression analysis. The closest agreement between measured and estimated LAI values was achieved when using models based on a combination of an SVI and a texture parameter (adjusted $r^2 = 0.84$).

Table 4. Results obtained when using both SVIs and texture parameters.

Variance	Model	r^2_{adj}	RMSE
CON_W5×5 + DVI	$y = 0.18e^{0.22x}$	0.44	1.00
CON_W5×5 + EVI	$y = 0.33e^{0.24x}$	0.63	0.97
CON_W5×5 + NLI	$y = 0.50e^{0.25x}$	0.64	0.79
CON_W5×5 + MSAVI	$y = 0.53e^{0.28x}$	0.72	0.90
CON_W5×5 + NDVI	$y = 0.63e^{0.25x}$	0.72	0.90
CON_W5×5 + SAVI	$y = 1.17e^{0.22x}$	0.65	0.93
DIS_W9×9 + DVI	$y = 0.11e^{0.22x}$	0.44	0.84
DIS_W9×9 + EVI	$y = 0.23x^{0.59}$	0.58	0.81
DIS_W9×9 + NLI	$y = 0.54x^{0.13}$	0.63	0.74
DIS_W9×9 + MSAVI	$y = 0.52e^{0.15x}$	0.70	0.64
DIS_W9×9 + NDVI	$y = 0.53x^{0.50}$	0.76	0.85
DIS_W9×9 + SAVI	$y = 0.99e^{0.13x}$	0.58	0.73
ENT_W3×3 + EVI	$y = 0.72x^{0.18}$	0.24	1.09
ENT_W3×3 + NLI	$y = 1.12x^{0.26}$	0.69	0.72
ENT_W3×3 + MSAVI	$y = 1.16x^{0.26}$	0.64	0.81
ENT_W3×3 + NDVI	$y = 1.31x^{0.22}$	0.49	0.97
ENT_W3×3 + SAVI	$y = 2.51e^{0.047x}$	0.23	1.10
HOM_W3×3 + DVI	$y = 0.41e^{-0.17x}$	0.71	0.91
HOM_W3×3 + EVI	$y = 0.41e^{-0.17x}$	0.71	0.62
HOM_W3×3 + NLI	$y = 0.87e^{-0.068x}$	0.68	0.66
HOM_W3×3 + MSAVI	$y = 1.04e^{-0.098x}$	0.76	0.55
HOM_W3×3 + NDVI	$y = 1.07e^{-0.091x}$	0.69	0.54
HOM_W3×3 + SAVI	$y = 1.94e^{-0.10x}$	0.75	0.51
ASM_W5×5 + DVI	$y = 0.15e^{-2.27x}$	0.84	0.54
ASM _W5×5 + EVI	$y = 0.27e^{-0.24x}$	0.83	0.60
ASM _W5×5 + NLI	$y = 0.31e^{-0.034x}$	0.77	0.51
ASM_W5×5 + MSAVI	$y = 0.34e^{-0.038x}$	0.84	0.41
ASM _W5×5 + NDVI	$y = 0.43e^{-0.21x}$	0.82	0.47
ASM _W5×5 + SAVI	$y = 0.76e^{-0.21x}$	0.83	0.43
VAR_W3×3 + DVI	$y = 0.092e^{0.19x}$	0.51	1.03
VAR_W3×3 + EVI	$y = 0.14e^{0.23x}$	0.66	0.72
VAR_W3×3 + NLI	$y = 0.24e^{0.24x}$	0.71	0.74
VAR_W3×3 + MSAVI	$y = 0.29e^{0.21x}$	0.75	0.74
VAR_W3×3 + NDVI	$y = 0.30e^{0.23x}$	0.72	0.78
VAR_W3×3 + SAVI	$y = 0.58e^{0.20x}$	0.70	0.86
COR_W5×5 + DVI	$y = -0.49 + 0.45x - 0.10x^2$	0.71	0.73
COR_W5×5 + EVI	$y = -0.99 + 0.92x - 0.21x^2$	0.72	0.53
COR_W5×5 + NLI	$y = -2.56 + 2.15x - 0.44x^2$	0.72	0.80
COR_W5×5 + MSAVI	$y = -2.34 + 2.01x - 0.42x^2$	0.73	0.78
COR_W5×5 + NDVI	$y = -1.89 + 1.28x - 0.38x^2$	0.69	0.73
COR_W5×5 + SAVI	$y = -3.26 + 2.76x - 0.61x^2$	0.73	0.92

Note: The variables x and y in the above expressions represent the field LAI measurements and the estimates obtained using the specified combinations of SVI and texture parameter, respectively. All adjusted r^2 values are statistically significantly at the 0.99 confidence level. RMSE values were calculated based on the differences between measured and predicted LAI values.

5.1. *Relationship between LAIs and SVIs*

The lower adjusted r^2 value (0.68) obtained for SVIs may be due to the high LAI values for the study area. Many SVIs become 'saturated' above a certain LAI threshold (which typically occurs at LAI values of 3–5). Consequently, they will grossly underestimate the LAI values for high biomass forests (Turner et al. 1999; Jensen et al. 2008; Yang et al.

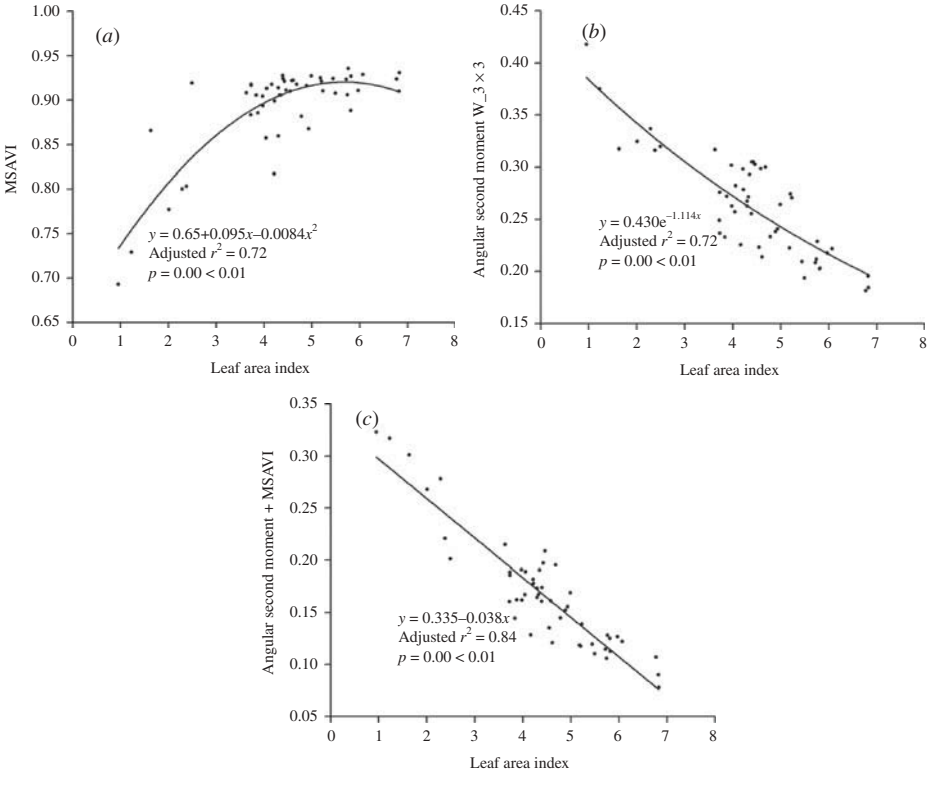

Figure 5. Scatter plots showing the best results achieved using (*a*) SVIs, (*b*) texture parameters, and (*c*) SVIs and texture parameters in combination.

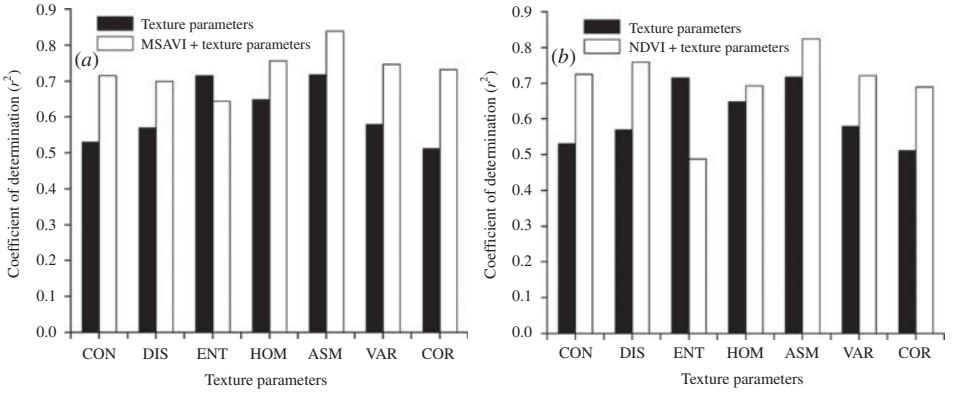

Figure 6. Agreement between predicted and measured LAI values achieved using (*a*) MSAVI alone; (*b*) angular second moment parameter (W_3×3) alone; and (*c*)) MSAVI and angular second moment parameter (W_3×3) in combination.

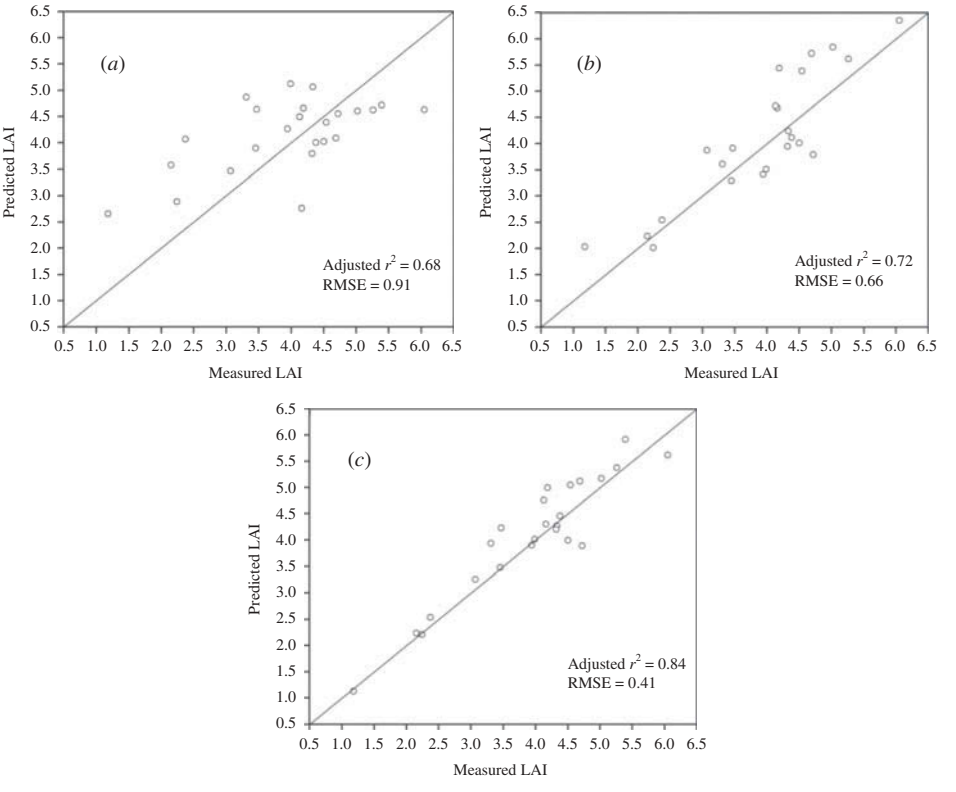

Figure 7. Coefficients of determination (r^2) for LAI retrieval using combinations of two SVIs with texture parameters and using texture parameters alone.

2012). This constitutes one of the principal limitations on the use of remote sensing for measuring the LAI of forest canopies (Davi et al. 2006). Wulder (1998) reported that the relationship between NDVI and LAI may be reduced by variation in age class, height, stand density, and crown closure. The heterogeneity of forest might weaken the LAI–SVI relationship (Colombo et al. 2003). Previous studies have demonstrated that models based on SVI analysis of Quickbird images do not provide reliable estimates of LAI, yielding adjusted r^2 values of only 0.42 (Lin et al. 2008) and 0.50 (Jensen et al. 2008). In this research, we tested eight commonly used SVIs in order to assess the potential of spectral information from Quickbird data used for LAI estimation. Although some complex SVIs (e.g. MSAVI, SAVI, and NDVI) performed better than single spectral bands (b1, b2, and b3), simple ratio (SR) and atmospherically resistant vegetation index (ARVI) performed poorly.

5.2. Relationship between LAI and image texture

The best r^2 value for a model based on a texture parameter was 0.72, which is higher than that achieved for a model based on MSAVI (0.68). Analyses based on texture parameters were thus better than SVI analyses for estimating LAI values in black locust plantations based on remote-sensing data. This may be due to the high resolution of the panchromatic Quickbird images used for textural analysis, which increases the scope for distinguishing

specific forest structures (Aguera, Aguilar, and Aguilar 2008; Franklin et al. 2000; Kabir et al. 2010; Ota, Mizoue, and Yoshida 2011). In contrast to previous reports on estimation of LAI values using texture statistics (Wulder et al. 1998), this work used simple linear and nonlinear models involving single texture parameters. Nevertheless, we still achieved significant improvements in the quality of the LAI estimates obtained, and we also identified specific texture parameters (angular second moment and entropy parameters) and window sizes (3 × 3 and 5 × 5) most suitable for estimating LAI values. These results contradict the findings of Colombo et al. (2003), who reported that the best textural indicator for this purpose was the dissimilarity index, computed using a 6 × 6 pixel window. Window size influences the resultant texture, possibly due to the amount of variance included (Wulder et al. 1998). Small window sizes were more sensitive to inter-pixel differences in the proportions of tree crown and shadow, whereas a larger window may not extract texture information efficiently due to over-smoothing of texture variation (Fuchs et al. 2009; Sarker and Nichol 2011).

When texture is decomposable, it has two basic dimensions by which it may be described (Haralick 1979). The first is for describing the primitives out of which the image texture is composed – for example, angular second moment, homogeneity, and entropy. The second dimension is for the description of spatial dependence or interaction between the primitives of texture – for example, dissimilarity, mean, and correlation (Haralick 1979; Wulder et al. 1998). The fact that angular second moment, entropy, and homogeneity perform better may be attributed to variation in texture dimensions.

5.3. *Relationship of LAIs and SVIs with texture parameters*

The most accurate model among those considered in this work is based on a combination of SVIs and a texture parameter, and yielded an adjusted r^2 value of 0.84. A similar approach has previously been used to improve the accuracy of forest biomass estimates (Nichol and Sarker 2011), LAI retrieval for different vegetation types (Colombo et al. 2003) and urban forests (Gu et al. 2012), and the accuracy of forest type classification (Ota, Mizoue, and Yoshida 2011). However, it has not been widely used to retrieve LAI data for forests in mountain areas such as the Loess Plateau.

Texture can represent differences in forest stand structure and provide information concerning the physical distribution of scene elements (Wulder et al. 1998; Fuch et al. 2009), while vegetation indices can provide information about vegetation content. The combination of spatial and spectral information is a surrogate for actual forest structural and vegetation information (Wulder, Franklin, and Lavigne 1996; Wulder et al. 1998). As demonstrated in this research, a combination of spectral and spatial characteristics can be used to build a reliable model for estimation of LAI values of black locust plantations. When the LAI value of forest was larger than 3, the spectral information could not represent the complex assemblage of structural characteristics. Moreover, it has not previously been possible to derive sufficient spectral information from remote-sensing images of such areas due to factors such as shadows, foliage height, and stand density (Wood et al. 2012). The outstanding improvement in the adjusted r^2 when adding textural information might be explained by the non-uniform and non-radom spatial distribution of black locust plantations. Forest is a mosaic of dense and sparse vegetation cells and the complex structure can be determined by considering texture parameters when working with images of high spatial resolution (Wulder 1998; Colombo et al. 2003; Gebreslasie, Ahmed, and van Aardt 2011; Wood et al. 2012). Colomobo (2003) reported that when the spectral information is heterogeneous and patchy, texture information is useful. In our

study, adding texture information to spectral information improved LAI estimation accuracy. This might be related to the heterogeneous forest structure of black locust plantation, where trees have a clumped distribution. The black locust has a clumped distribution pattern due to asexual reproduction (Call and Nilsen 2003). Liesebach and Schneck (2004) have claimed that after the first establishment of a black locust population, it is more likely that asexual reproduction will dominate for many generations.

6. Conclusions

The potential of Quickbird imagery for LAI estimation was explored and high model performance was obtained by using a combination of angular second moment and MSAVI in the present study. The promising results (adjusted r^2= 0.84, RMSE = 0.41) indicated that the combination of texture and SVIs has enhanced potential for LAI estimation in comparison with other image processing techniques. Texture proved to be more effective than spectral information for LAI estimation based on Quickbird data. This improved performance may be due to the higher resolution (0.6m) of Quickbird data and the large number of field samples. However, the present work was conducted based on commonly used SVIs and texture algorithms. Future work will focus on testing different texture algorithms and other SVIs for the same task of LAI estimation. Furthermore, estimation of LAI will require the combination of other spatial variables with spectral information. In this respect, we suggest that optical sensors should be integrated with lidar data in order to provide vertical spectral and spatial information on forest vegetation.

Funding

This research was financed under the auspices of the twelfth Five-Year Plan of National Science and Technology in China, in the form of a grant to Z.Z. [grant number 2012BAD22B0302] and the programme of Silviculture teaching reform [grant number Z105021003].

Acknowledgements

We thank the anonymous reviewers for their constructive and valuable comments, and the editors for their assistance in refining this article. We also thank Wang Cheng from Northwest A&F University for providing valuable suggestions during manuscript revision.

References

Aguera, F., F. J. Aguilar, and M. A. Aguilar. 2008. "Using Texture Analysis to Improve Per-Pixel Classification of Very High Resolution Images for Mapping Plastic Greenhouses." *ISPRS Journal of Photogrammetry and Remote Sensing* 63 (6): 635–646. doi:10.1016/j.isprsjprs.2008.03.003.

Asner, G. P., C. A. Bateson, J. L. Privette, N. El Saleous, and C. A. Wessman. 1998. "Estimating Vegetation Structural Effects on Carbon Uptake Using Satellite Data Fusion and Inverse Modeling." *Journal of Geophysical Research-Atmospheres* 103 (D22): 28839–28853. doi:10.1029/98jd02459.

Boyd, D. S. 1999. "The Relationship Between the Biomass of Cameroonian Tropical Forests and Radiation Reflected in Middle Infrared Wavelengths (3.0–5.0 Mu m)." *International Journal of Remote Sensing* 20 (5): 1017–1023.

Burner, D. M., H. Pote, and A. Ares. 2005. "Management Effects on Biomass and Foliar Nutritive Value of *Robinia pseudoacacia* and *Gleditsia triacanthos f. inermis* in Arkansas, USA." *Agroforestry Systems* 65 (3): 207–214. doi:10.1007/s10457-005-0923-9.

Call, L. J., and E. T. Nilsen. 2003. "Analysis of Spatial Patterns and Spatial Association Between the Invasive Tree-of-Heaven (*Ailanthus altissima*) and the Native Black Locust (*Robinia pseudoacacia*)." *The American Midland Naturalist* 150 (1): 1–14.

Canisius, F., and R. Fernandes. 2012. "ALOS PALSAR L-Band Polarimetric SAR Data and In Situ Measurements for Leaf Area Index Assessment." *Remote Sensing Letters* 3 (3): 221–229. doi:10.1080/01431161.2011.559288.

Cao, S., Li. Chen, and X. Yu. 2009. "Impact of China's Grain for Green Project on the Landscape of Vulnerable Arid and Semi-Arid Agricultural Regions: A Case Study in Northern Shaanxi Province." *Journal of Applied Ecology* 46 (3): 536–543. doi:10.1111/j.1365-2664.2008.01605.x.

Chason, J. W., D. D. Baldocchi, and M. A. Huston. 1991. "A Comparison of Direct and Indirect Methods for Estimating Forest Canopy Leaf Area." *Agricultural and Forest Meteorology* 57 (1–3): 107–128.

Chen, J. M., and J. Cihlar. 1996. "Retrieving Leaf Area Index of Boreal Conifer Forests Using Landsat TM Images." *Remote Sensing of Environment* 55 (2): 153–162.

Colombo, R., D. Bellingeri, D. Fasolini, and C. M. Marino. 2003. "Retrieval of Leaf Area Index in Different Vegetation Types Using High Resolution Satellite Data." *Remote Sensing of Environment* 86 (1): 120–131. doi:10.1016/s0034-4257(03)00094-4.

Davi, H., K. Soudani, T. Deckx, E. Dufrene, V. Le Dantec, and C. Francois. 2006. "Estimation of Forest Leaf Area Index from SPOT Imagery Using NDVI Distribution over Forest Stands." *International Journal of Remote Sensing* 27 (5–6): 885–902. doi:10.1080/01431160500227896.

Fassnacht, K. S., S. T. Gower, M. D. MacKenzie, E. V. Nordheim, and T. M. Lillesand. 1997. "Estimating the Leaf Area Index of North Central Wisconsin Forests Using the Landsat Thematic Mapper." *Remote Sensing of Environment* 61 (2): 229–245.

Franklin, S. E., R. J. Hall, L. M. Moskal, A. J. Maudie, and M. B. Lavigne. 2000. "Incorporating Texture into Classification of Forest Species Composition from Airborne Multispectral Images." *International Journal of Remote Sensing* 21 (1): 61–79.

Franklin, S. E., M. A. Wulder, and M. B. Lavigne. 1996. "Automated Derivation of Geographic Window Sizes for Use in Remote Sensing Digital Image Texture Analysis." *Computers & Geosciences* 22 (6): 665–673. doi:10.1016/0098-3004(96)00009-x.

Fu, Z., J. L. Jindi Wang, H. M. Song, Y. P. Zhou, and B. S. Chen. 2011. "Estimation of Forest Canopy Leaf Area Index Using MODIS, MISR, and LiDAR Observations." *Journal of Applied Remote Sensing* 5. doi:05353010.1117/1.3594171.

Fuchs, H., P. Magdon, C. Kleinn, and H. Flessa. 2009. "Estimating Above Ground Carbon in a Catchment of the Siberian Forest Tundra: Combining Satellite Imagery and Field Inventory." *Remote Sensing of Environment* 113 (3): 518–531. doi:10.1016/j.rse.2008.07.017.

GCOS. 2006. "Systematic Observation Requirements for Satellite Based Products for Climate." Supplemental Details to the Satellite Based Component of the Implementation Plan for the Global Observing System for Climate in Support of the UNFCCC. GCOS Rep. GCOS-107 and WMO/TD 1338, 103 pp. Geneva: GCOS.

Gebreslasie, M. T., F. B. Ahmed, and J. A. N. van Aardt. 2011. "Extracting Structural Attributes from IKONOS Imagery for Eucalyptus Plantation Forests in KwaZulu-Natal, South Africa, Using Image Texture Analysis and Artificial Neural Networks." *International Journal of Remote Sensing* 32 (22): 7677–7701. doi:10.1080/01431161.2010.527392.

Goel, N. S., and W. Qin. 1994. "Influences of Canopy Architecture on Relationships Between Various Vegetation Indices and LAI and FPAR: A Computer Simulation." *Remote Sensing Reviews* 10 (4): 309–347.

Gong, P., R. Pu, G. S. Biging, and M. R. Larrieu. 2003. "Estimation of Forest Leaf Area Index Using Vegetation Indices Derived from Hyperion Hyperspectral Data." *IEEE Transactions on Geoscience and Remote Sensing* 41 (6): 1355–1362.

Gray, J., and C. Song. 2012. "Mapping Leaf Area Index Using Spatial, Spectral, and Temporal Information from Multiple Sensors." *Remote Sensing of Environment* 119 (16): 173–183.

Gu, Z., W. Ju, Y. Liu, D. Li, and W. Fan. 2012. "Applicability of Spectral and Spatial Information from IKONOS-2 Imagery in Retrieving Leaf Area Index of Forests in the Urban Area of Nanjing, China." *Journal of Applied Remote Sensing* 6. doi:10.1117/1.jrs.6.063556.

Haralick, R. M. 1979. "Statistical and Structural Approaches to Texture." *Proceedings of the IEEE* 67 (5): 786–804.

Haralick, R. M., K. Shanmugam, and I. H. Dinstein. 1973. "Textural Features for Image Classification." *IEEE Transactions on Systems, Man and Cybernetics* 6: 610–621.
Huete, A. R. 1988. "A Soil-Adjusted Vegetation Index (SAVI)." *Remote Sensing of Environment* 25 (3): 295–309.
Huete, A. R., R. D. Jackson, and D. F. Post. 1985. "Spectral Response of a Plant Canopy with Different Soil Backgrounds." *Remote Sensing of Environment* 17 (1): 37–53.
Huete, A., C. Justice, and H. Liu. 1994. "Development of Vegetation and Soil Indices for MODIS-EOS." *Remote Sensing of Environment* 49 (3): 224–234.
Jensen, J. L. R., K. S. Humes, L. A. Vierling, and A. T. Hudak. 2008. "Discrete Return Lidar-Based Prediction of Leaf Area Index in Two Conifer Forests." *Remote Sensing of Environment* 112 (10): 3947–3957.
Jonckheere, I., S. Fleck, K. Nackaerts, B. Muys, P. Coppin, M. Weiss, and F. Baret. 2004. "Review of Methods for In Situ Leaf Area Index Determination – Part I. Theories, Sensors and Hemispherical Photography." *Agricultural and Forest Meteorology* 121 (1–2): 19–35. doi:10.1016/j.agrformet.2003.08.027.
Jordan, C. F. 1969. "Derivation of Leaf-Area Index from Quality of Light on the Forest Floor." *Ecology* 50: 663–666.
Kabir, S., D. C. He, M. A. Sanusi, and W. Hussin. 2010. "Texture Analysis of IKONOS Satellite Imagery for Urban Land Use and Land Cover Classification." *Imaging Science Journal* 58 (3): 163–170. doi:10.1179/136821909x12581187860130.
Kaufman, Y. J., and D. Tanre. 1992. "Atmospherically Resistant Vegetation Index (ARVI) for EOS-MODIS." *Geoscience and Remote Sensing, IEEE Transactions on* 30 (2): 261–270.
Kayitakire, F., C. Hamel, and P. Defourny. 2006. "Retrieving Forest Structure Variables Based on Image Texture Analysis and IKONOS-2 Imagery." *Remote Sensing of Environment* 102 (3–4): 390–401. doi:10.1016/j.rse.2006.02.022.
Korhonen, L., I. Korpela, J. Heiskanen, and M. Maltamo. 2011. "Airborne Discrete-Return LIDAR Data in the Estimation of Vertical Canopy Cover, Angular Canopy Closure and Leaf Area Index." *Remote Sensing of Environment* 115 (4): 1065–1080. doi:10.1016/j.rse.2010.12.011.
Liesebach, H., and V. Schneck. 2004. "Genetic Diversity and Differentiation in a Black Locust (Robinia Pseudoacacia L.) Progeny Test." *International Journal of Forest Genetics* 11: 151–161.
Lin, W. –P., M. Zhao, Y. –F. Zhang, Y. –L. Liu, D. –Y. Liu, and J. Gao. 2008. "Study on Estimation of Urban Forest LAI Models Based on SPOT5." *Science of Surveying and Mapping* 2 023.
Lu, D. 2006. "The Potential and Challenge of Remote Sensing-Based Biomass Estimation." *International Journal of Remote Sensing* 27 (7): 1297–1328.
Luo, W. X. 1995. *Study on the Construction of Ecological Economy Protection Forest System on Weibei Loess Plateau*. Beijing: Chinese Forestry Publishing Housing.
Marceau, D. J., P. J. Howarth, J. -M. M. Dubois, and D. J. Gratton. 1990. "Evaluation of the Grey-Level Co-Occurrence Matrix Method for Land-Cover Classification Using SPOT Imagery." *IEEE Transactions on Geoscience and Remote Sensing* 28 (4): 513–519.
Mather, P. M. 1999. *Computer Processing of Remote Sensing Images*. New York: Wiley.
Muukkonen, P., and J. Heiskanen. 2005. "Estimating Biomass for Boreal Forests Using ASTER Satellite Data Combined with Standwise Forest Inventory Data." *Remote Sensing of Environment* 99 (4): 434–447.
Nichol, J. E., and Md. L. R. Sarker. 2011. "Improved Biomass Estimation Using the Texture Parameters of Two High-Resolution Optical Sensors." *IEEE Transactions on Geoscience and Remote Sensing* 49 (3): 930–948. doi:10.1109/tgrs.2010.2068574.
Ota, T., N. Mizoue, and S. Yoshida. 2011. "Influence of Using Texture Information in Remote Sensed Data on the Accuracy of Forest Type Classification at Different Levels of Spatial Resolution." *Journal of Forest Research* 16 (6): 432–437. doi:10.1007/s10310-010-0233-6.
Ozdemir, I., and A. Karnieli. 2011. "Predicting Forest Structural Parameters Using the Image Texture Derived from WorldView-2 Multispectral Imagery in a Dryland Forest, Israel." *International Journal of Applied Earth Observation and Geoinformation* 13 (5): 701–710. doi:10.1016/j.jag.2011.05.006.
Peng, Li., Z. Zhong, and Li. Zhan-bin. 2004. "Vertical Root Distribution Characters of *Robinia pseudoacacia* on the Loess Plateau in China." *Journal of Forestry Research* 15 (2): 87–92.

Pu, R. 2012. "Mapping Leaf Area Index over a Mixed Natural Forest Area in the Flooding Season Using Ground-Based Measurements and Landsat TM Imagery." *International Journal of Remote Sensing* 33 (20): 6600–6622. doi:10.1080/01431161.2012.692887.

Qi, J., A. Chehbouni, A. R. Huete, Y. H. Kerr, and S. Sorooshian. 1994. "A Modified Soil Adjusted Vegetation Index." *Remote Sensing of Environment* 48 (2): 119–126. doi:10.1016/0034-4257(94)90134-1.

Richardson, A. J., and C. L. Weigand. 1977. "Distinguishing Vegetation from Soil Background Information." *Photogrammetric Engineering and Remote Sensing* 43 (12): 1541–1552.

Rouse, J. W., R. H. Haas, J. A. Schell, and D. W. Deering. 1974. "Monitoring Vegetation Systems in the Great Plains with ERTS." *NASA Special Publication* 351:309–317.

Sarker, L. R., and J. E. Nichol. 2011. "Improved Forest Biomass Estimates Using ALOS AVNIR-2 Texture Indices." *Remote Sensing of Environment* 115 (4): 968–977. doi:10.1016/j.rse.2010.11.010.

Shin, Y. H., M. Seguchi, M. Koriyama, and A. Isnansetyo. 2010. "Estimation of LAI in the Forested Watershed Using ASTER Data Based on Price's Model in Summer and Winter." *European Journal of Forest Research* 129 (6): 1237–1245. doi:10.1007/s10342-010-0414-z.

Solana-Arellano, E., H. Echavarria-Heras, and M. G. Martinez. 2003. "Improved Leaf Area Index Based Biomass Estimations for *Zostera marina* L." *Mathematical Medicine and Biology: A Journal of the IMA* 20 (4): 367–375. doi:10.1093/imammb/20.4.367.

Soudani, K., C. Francois, G. le Maire, V. Le Dantec, and E. Dufrene. 2006. "Comparative Analysis of IKONOS, SPOT, and ETM+ Data for Leaf Area Index Estimation in Temperate Coniferous and Deciduous Forest Stands." *Remote Sensing of Environment* 102 (1–2): 161–175. doi:10.1016/j.rse.2006.02.004.

Thomas, V., T. Noland, P. Treitz, and J. H. McCaughey. 2011. "Leaf Area and Clumping Indices for a Boreal Mixed-Wood Forest: Lidar, Hyperspectral, and Landsat Models." *International Journal of Remote Sensing* 32 (23): 8271–8297. doi:10.1080/01431161.2010.533211.

Tobin, B., K. Black, B. Osborne, B. Reidy, T. Bolger, and M. Nieuwenhuis. 2006. "Assessment of Allometric Algorithms for Estimating Leaf Biomass, Leaf Area Index and Litter Fall in Different-Aged Sitka Spruce Forests." *Forestry* 79 (4): 453–465. doi:10.1093/forestry/cpl030.

Tuominen, S., and A. Pekkarinen. 2005. "Performance of Different Spectral and Textural Aerial Photograph Features in Multi-Source Forest Inventory." *Remote Sensing of Environment* 94 (2): 256–268.

Turner, D. P., W. B. Cohen, R. E. Kennedy, K. S. Fassnacht, and J. M. Briggs. 1999. "Relationships Between Leaf Area Index and Landsat TM Spectral Vegetation Indices Across Three Temperate Zone Sites." *Remote Sensing of Environment* 70 (1): 52–68. doi:10.1016/s0034-4257(99)00057-7.

Wang, Y., Z. Xie, S. S. Malhi, C. L. Vera, Y. Zhang, and J. Wang. 2009. "Effects of Rainfall Harvesting and Mulching Technologies on Water Use Efficiency and Crop Yield in the Semi-Arid Loess Plateau, China." *Agricultural Water Management* 96 (3): 374–382.

Wei, G., W. Chen, W. Zhu, J. Chun Chen, P. W. Young, and C. Bontemps. 2009. "Invasive Robinia Pseudoacacia in China Is Nodulated by *Mesorhizobium* and *Sinorhizobium* Species That Share Similar Nodulation Genes with Native American Symbionts." *FEMS Microbiology Ecology* 68 (3): 320–328. doi:10.1111/j.1574-6941.2009.00673.x.

Wolter, P. T., P. A. Townsend, and B. R. Sturtevant. 2009. "Estimation of Forest Structural Parameters Using 5 and 10 Meter SPOT-5 Satellite Data." *Remote Sensing of Environment* 113 (9): 2019–2036. doi:10.1016/j.rse.2009.05.009.

Wood, E. M., A. M. Pidgeon, V. C. Radeloff, and N. S. Keuler. 2012. "Image Texture as a Remotely Sensed Measure of Vegetation Structure." *Remote Sensing of Environment* 121: 516–526. doi:10.1016/j.rse.2012.01.003.

Wulder, M. 1998. "Optical Remote-Sensing Techniques for the Assessment of Forest Inventory and Biophysical Parameters." *Progress in Physical Geography* 22 (4): 449–476. doi:10.1191/030913398675385488.

Wulder, M. A., S. E. Franklin, and M. B. Lavigne. 1996. "High Spatial Resolution Optical Image Texture for Improved Estimation of Forest Stand Leaf Area Index." *Canadian Journal of Remote Sensing* 22 (4): 441–449.

Wulder, M. A., E. F. LeDrew, S. E. Franklin, and M. B. Lavigne. 1998. "Aerial Image Texture Information in the Estimation of Northern Deciduous and Mixed Wood Forest Leaf Area Index (LAI)." *Remote Sensing of Environment* 64 (1): 64–76.

Yang, F., J. L. Sun, H. L. Fang, Z. F. Yao, J. H. Zhang, Y. Q. Zhu, K. S. Song, Z. M. Wang, and M. G. Hu. 2012. "Comparison of Different Methods for Corn LAI Estimation over Northeastern China." *International Journal of Applied Earth Observation and Geoinformation* 18: 462–471. doi:10.1016/j.jag.2011.09.004.

Yuan, Jin-guo, Zheng Niu, and Xi-ping Wang. 2009. "Atmospheric Correction of Hyperion Hyperspectral Image Based on FLAASH." *Spectroscopy and Spectral Analysis* 29 (5): 1181–1185. doi:10.3964/j.issn.1000-0593(2009)05-1181-05.

Zhao, F., Y. Xiaoyuan, M. A. Schull, M. O. Román-Colón, Y. Tian, W. Zhuosen, Z. Qingling, D. L. B. Jupp, J. L. Lovell, and D. S. Culvenor. 2011 . "Measuring Effective Leaf Area Index, Foliage Profile, and Stand Height in New England Forest Stands Using a Full-Waveform Ground-Based Lidar." *Remote Sensing of Environment* 115 (11): 2954–2964. doi:10.1016/j.rse.2010.08.030.

Zhong, Z., C. Xiangrong, X. Wenpeng, W. Dihai, and Y. Zhifa. 2006. "Difference of Fine Root Vertical Distribution of Robinia Pseudoacacia Under the Different Climate Regions in the Loess Plateau." *Scientia Silvae Sinicae* 42 (11): 1.